Determination of Accumulation of Molecules in *Escherichia coli*

George M. Ongwae[1], Zichen Liu[1], Mahendra D. Chordia[1], Brianna E. Dalesandro[1], Taijie Guo[2], Jiajia Dong[2], and Marcos M. Pires[1*]

[1]Department of Chemistry, University of Virginia

Charlottesville, VA 22904, USA

[2] Institute of Translational Medicine, Zhangjiang Institute for Advanced Study,

Shanghai Jiao Tong University

Shanghai 200232, China

* corresponding author: mpires@virginia.edu

Abstract

There is an urgent need for efficacious agents against Gram-negative bacterial pathogens because the presence of an outer membrane inherently reduces susceptibility to antibiotics. This asymmetric bilayer effectively diminishes the permeation of small molecules into bacterial cells. A significant complication to drug discovery and development is that few methods exist for measuring the permeation of molecules past the outer membrane. Our laboratory has bridged this technical gap by developing a robust assay to semi-quantitatively measure the accumulation of small molecules into Gram-negative bacteria. Our assay is based on anchoring bioorthogonal strained alkyne epitopes within HaloTag-expressing bacteria. Permeation is then gauged with azide-bearing test molecules in live cells following *in cyto* strain-promoted azide-alkyne cycloaddition (SPAAC). Overall, the Bacterial Azide Penetration Assay (BAPA) operates by semi-quantitatively measuring small molecule accumulation in a facile manner using reagents that are readily attainable, requiring basic instrumentation, and are compatible with high-throughput analysis. To this point, we have demonstrated that we can analyze the permeation of 1000+ molecules using BAPA.

Introduction

Gram-negative pathogens exhibit inherent resistance to antibiotics, primarily attributed to the distinctive structure of their cell walls. In addition to the conventional plasma membrane, Gram-negative bacteria possess an asymmetric outer membrane that effectively hinders the penetration of small molecules into the periplasmic space (**Fig. 1A**). This outer membrane presents a formidable obstacle to target-based screening endeavors. Compounds that successfully traverse the outer membrane generally fall into two categories.[1] One subset of molecules possess specific physicochemical properties, such as optimal molecular weight and hydrogen bond count, enabling passive diffusion across the outer membrane. Conversely, hydrophilic molecules, including β-lactam antibiotics, exploit porins embedded within the outer membrane to circumvent its non-polar regions.

Unfortunately, our understanding of the precise parameters governing the transformation of non-permeating compounds into active agents remains limited, impeding iterative redesign efforts. These parameters can, in addition, serve as filters to enhance the quality of small molecule libraries. Principally, the lack of easily accessible tools for quantifying the accumulation of small molecules within bacteria has hindered the comprehensive definition of these molecular descriptors.

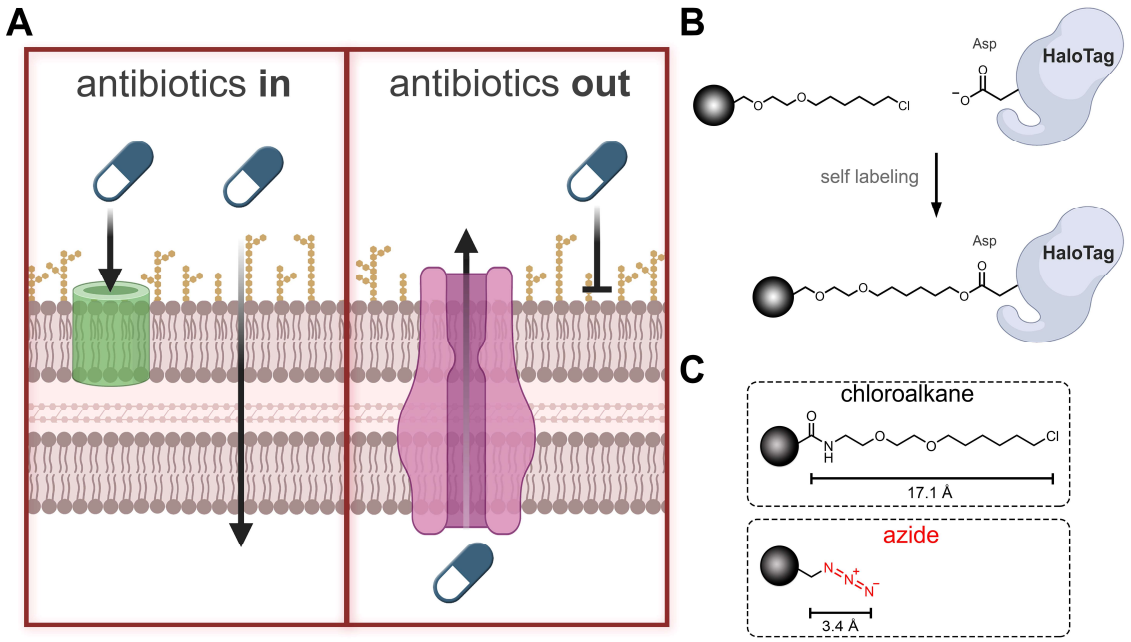

Figure 1. (**A**) The outer membrane of Gram-negative bacteria can pose a major challenge in the permeation of small molecules from the extracellular space to the periplasm and/or cytoplasm. (**B**) HaloTag promotes the covalent bond formation between the protein and the species attached to the chloroalkane tag. (**C**) Comparison of the sizes of the chloroalkane tag and the azide tag.

In the absence of facile methods to measure uptake of small molecules into bacterial cells, microbiologists have most often resorted to using antimicrobial activity (Minimum Inhibitory Concentration, MIC) as an approximation for drug accumulation. This approach has serious drawbacks because drug accumulation can be inherently independent from drug potency. Moreover, antivirulent agents or potentiators often lack antimicrobial activities and, therefore, cannot be subjected to MIC analyses. Recent efforts have demonstrated the utility of understanding what type of molecules accumulate most readily in *Escherichia coli* (*E. coli*) cells.[2] The Hergenrother laboratory analyzed a library of

molecules for their accumulation in *E. coli* K-12. This work culminated in the eNTRy rules, which highlight the role of primary amines in permeability.[3] Although mass spectrometry methodologies offer certain advantages, they also possess inherent limitations, including restricted throughput capacity and an inability to definitively ascertain cytosolic accumulation.

The current gold standard for molecule accumulation measurement in mammalian cells was recently developed by the Kritzer lab.[4] In the ChloroAlkane Penetration Assay (CAPA), HaloTag-expressing mammalian cells are pulse treated with chloroalkane-tagged test molecules followed by chloroalkane-fluorophore detection. HaloTags are routinely expressed as freely diffusing proteins in the cytoplasm or fused to organelle-homing proteins in mammalian cells[5], where they selectively and rapidly react with chloroalkanes to form a stable covalent bond (**Fig. 1B**). CAPA has been employed in various fields, including pharmaceutical research, to evaluate the permeability of drugs and other compounds, aiding in the development of effective delivery strategies.[4, 6] Our laboratory adopted the assay (Bacterial CAPA, BaCAPA) to measure the accumulation of small molecules in Gram-negative pathogens.[7]

Despite the wide adoption of CAPA in the measurement of molecule accumulation in mammalian systems[4, 6], we reasoned that the chloroalkane tag could still confound penetration analysis in bacteria. The chloroalkane tag is 15-atoms long and could potentially impact permeation profiles (**Fig. 1C**); in contrast, azides are generally considered to be the smallest and least disruptive biorthogonal tags.[8] To adopt BaCAPA

to function with azide-tagged test molecules, HaloTag-expressing bacterial cells can, instead, be treated with a molecule that converts the HaloTag anchor to a strained-alkyne; more specifically, HaloTags are tagged *in situ* with a dibenzocylcooctyne (DBCO) moiety linked to chloroalkane (**Fig. 2**). HaloTag-bound cyclooctynes can, then, be leveraged to gauge the access of azide-bearing test molecules following *in situ* strain-promoted azide-alkyne cycloaddition (SPAAC).[9]

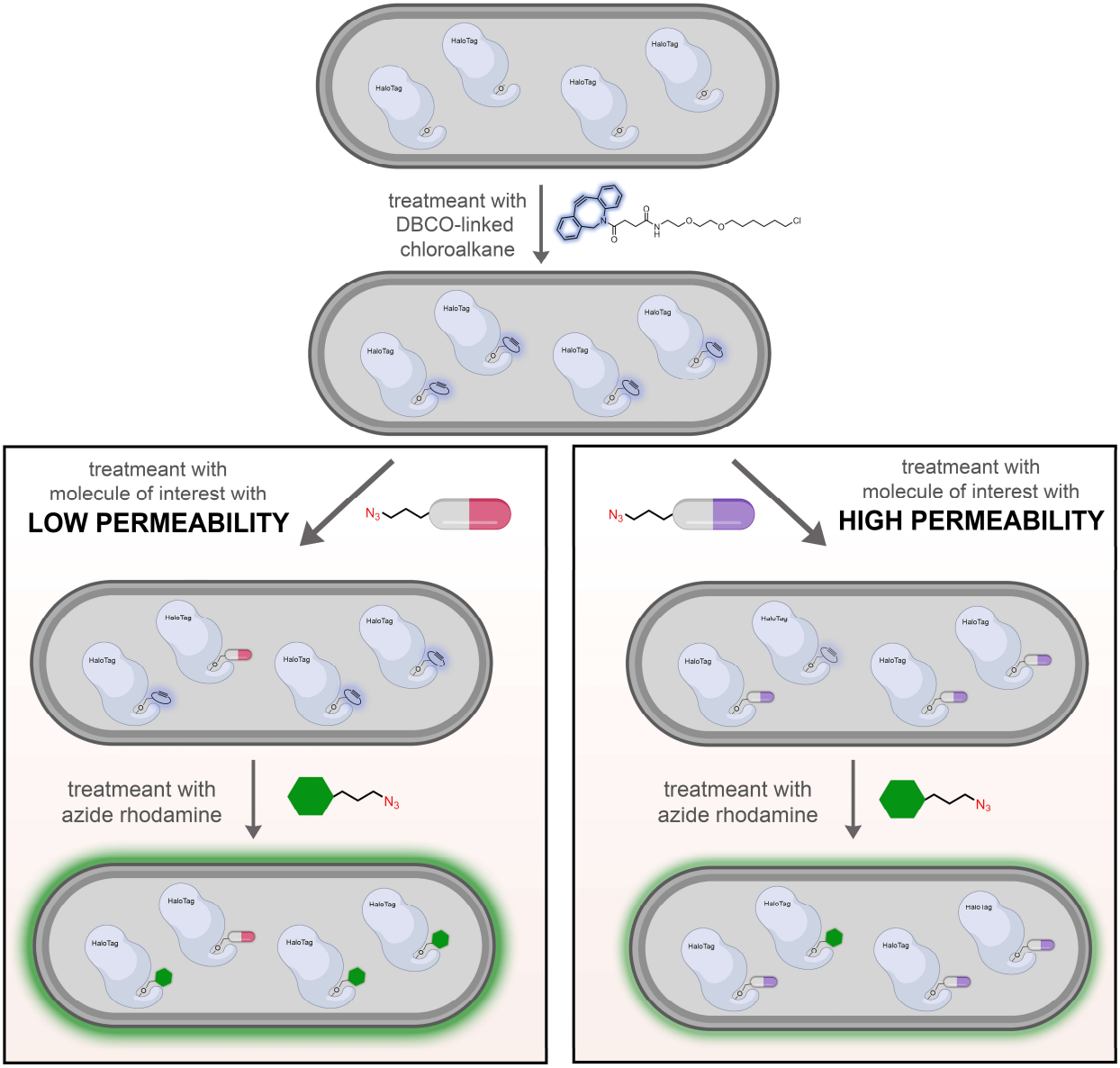

Figure 2. Assay workflow for BAPA. Gram-negative bacteria expressing HaloTag in the cytosol are treated with DBCO-linked chloroalkane. This treatment results in the anchoring of DBCO within HaloTag proteins. Next, the cells are treated with test molecules that are modified with an azide tag. A chase step follows in which cells are treated with an azide-tagged fluorophore. Ultimately, this competition assay results in cells with high fluorescence levels when treated with molecules having low permeability and low fluorescence levels when treated with highly permeable molecules.

To start, a plasmid was assembled for the expression of HaloTag based on a T5 promoter. *E. coli* (BW25113) was transformed with the plasmid and expression of HaloTag in *E. coli* was verified by treating cells with a chloroalkane-linked fluorophore (**R110cl**, **Fig. 3A**); cells were washed and analyzed by flow cytometry (**Fig. S1**). There was a 78-fold increase in cellular fluorescence from induced *E. coli* cells relative to uninduced cells (**Fig. 3B**). These results suggest that HaloTag expression was responsible for capturing the chloroalkane-linked fluorophore in the cytosol of *E. coli*. The cellular fluorescence level was also dependent on IPTG levels (**Fig. 3C**) and the concentration of **R110cl** (**Fig. 3D**). Confocal microscopy analysis of *E. coli* cells induced to express HaloTag and treated with **R110cl** revealed fluorescence staining throughout the cell, a finding that is consistent with cytosolic residence of this protein (**Fig. 3E**). Furthermore, fluorescence imaging of SDS-PAGE gel from cellular components of induced cells showed a fluorescent band in the expected molecular weight range (~30 kDa) of HaloTag (**Fig. 3D**). Together, these results establish that HaloTag can be used to specifically anchor molecules modified with a chloroalkane linker in *E. coli*.

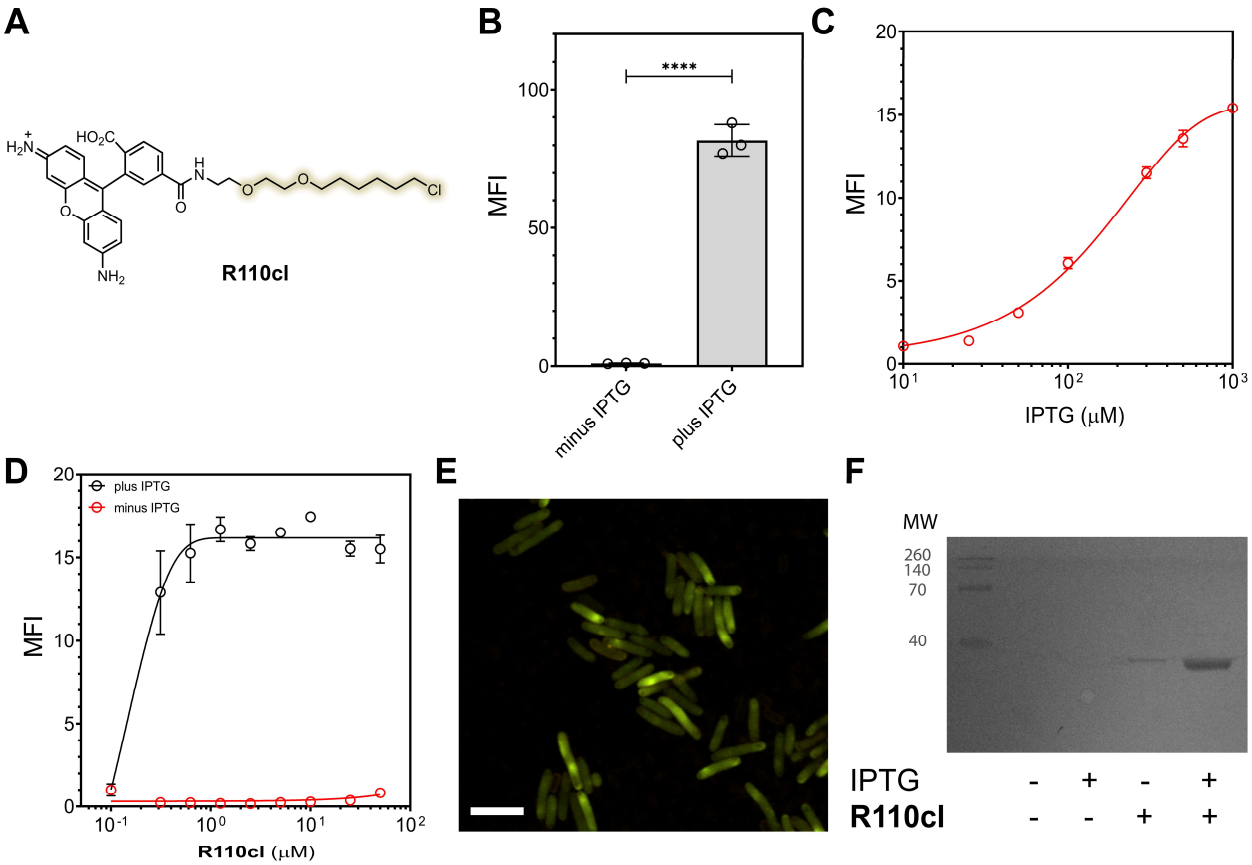

Figure 3. (**A**) Chemical structure of **R110cl**. (**B**) Flow cytometry analysis of *E. coli* treated with various concentrations of IPTG, followed by an incubation period with 5 μM of **R110cl**. (**C**) Flow cytometry analysis of *E. coli* treated with various concentrations of IPTG, followed by an incubation period with 5 μM of **R110cl**. (**D**) Flow cytometry analysis of *E. coli* treated with various concentrations of **R110cl** in the presence or absence of IPTG. (**E**) Confocal microscopy of *E. coli* cells that were induced with IPTG, both treated with 5 μM of **R110cl**; scale bar = 2 μm. (**F**) Fluorescence gel imaging analysis of cells that were treated 25 μM of DMSO or **R110cl**. Cellular contents were subjected to SDS-PAGE separation before being analyzed by a gel imager. The lines are non-linear fits of the data points. Data are represented as mean +/- SD (n = 3 independent samples in a single

experiment). *P*-values were determined by a two-tailed *t*-test (**** denotes a *p*-value < 0.0001).

We next set out to establish the feasibility of BAPA in reporting on the accumulation of azide-tagged molecules in the cytoplasm of *E. coli*. In batch, *E. coli* cells were induced to express HaloTag and incubated with chloroalkane-DBCO (**DBCOcl**) to install the reporter strained alkyne within the cytoplasm, and non-anchored molecules were removed by thoroughly washing the cells. To empirically determine the concentration to maximize DBCO anchoring, a BaCAPA-like experiment was performed whereby cells were pulsed with increasing concentrations of **DBCOcl** chased with **R110cl** (**Fig. 4A**). From our results, maximum levels of DBCO installation were reached with ~ 50 μM of **DBCOcl** with an EC_{50} of 18.5 μM. Several subsequent experiments were performed next to optimize the assay parameters. The first BAPA experiment was evaluated by treatment of *E. coli* with the azide-modified rhodamine (**R110az**) that should reveal the occupancy of DBCO handles within individual cells. Satisfyingly, a large dynamic range in fluorescence was observed (30-fold) in cells treated with both **DBCOcl** and **R110az** (**Fig. 4B**). In the absence of **DBCOcl** treatment, cellular fluorescence levels were similar to untreated cells, which indicates that **R110az** has little background staining levels. Cellular fluorescence levels were also near background in non-induced cells that were also treated with **DBCOcl** and **R110az**, indicating negligible retention of **DBCOcl** or cytosolic DBCO modified with **R110az**.

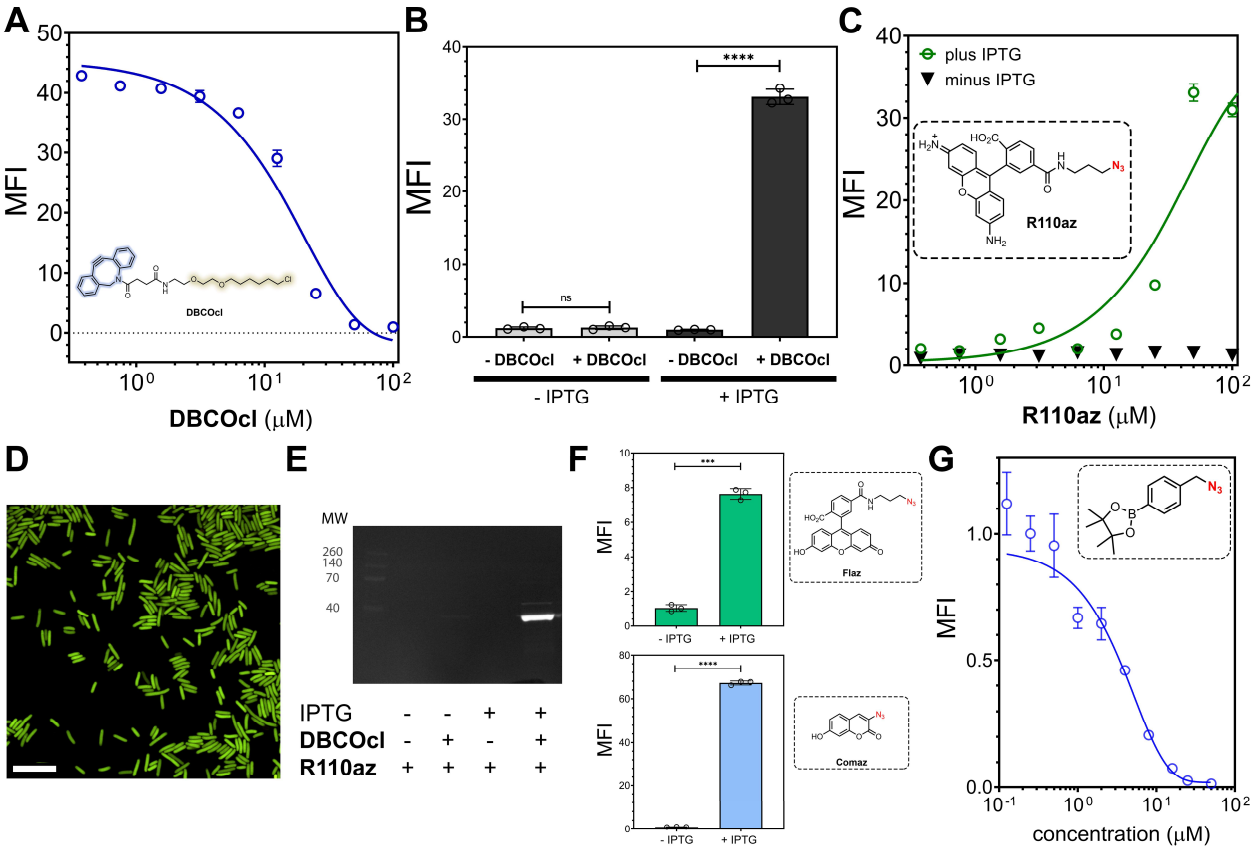

Figure 4. (**A**) Concentration dependency of **DBCOcl** in *E. coli* expressing HaloTag. Cells were pulse treated with **DBCOcl** followed by 25 μM of **R110cl** and analyzed by flow cytometry. (**B**) Flow cytometry analysis of *E. coli* in the presence/absence of **DBCOcl** and in the presence/absence of IPTG. (**C**) Flow cytometry analysis of *E. coli* treated with various concentrations of **R110az** in the chase step. (**D**) Confocal microscopy of *E. coli* cells that were induced with IPTG treated with 25 μM of **DBCOcl** followed by 25 μM of **R110az**; scale bar = 6 μm. (**E**) Fluorescence gel imaging analysis of cells that were pulse treated with/without **DBCOcl** followed by 25 μM of DMSO or **R110az**. Cellular contents were subjected to SDS-PAGE separation before being analyzed by a gel imager. (**F**) Flow cytometry analysis of BAPA with *E. coli* with two additional dyes, **Flaz** and **Comaz**. (**G**) BAPA analysis of a test azide-bearing small molecule analyzed by flow cytometry. The

lines are non-linear fits of the data points. Data are represented as mean +/- SD (n = 3 independent samples in a single experiment). *P*-values were determined by a two-tailed *t*-test (*** denotes a *p*-value < 0.001, **** < 0.0001, ns = not significant).

A concentration scan of **R110az** demonstrated that a large dynamic range was observed and established the concentration of **R110az** for all subsequent experiments (**Fig. 4C**). Confocal microscopy was consistent with fluorescence signals throughout the entire cell (**Fig. 4D**) and fluorescent gel imaging also showed that a band matching the molecular weight of HaloTag (**Fig. 4E**). Additionally, we evaluated the feasibility of employing BAPA in a smooth *E. coli* strain (ATCC 25922), which possesses intact lipopolysaccharides (LPS) on its outer surface. Smooth *E. coli* strains potentially have altered permeability profiles owing to the contributions that O-antigens may have in sterically shielding the porins.[10]. Satisfyingly, a similar dynamic range was also observed in an IPTG-dependent manner in smooth *E. coli* (**Fig. S1**). To demonstrate the ability of BAPA to monitor the permeation of molecules into *E. coli*, cells were titrated with a test azide-bearing molecule (**Fig. 4E**). A concentration-dependent decrease in cellular fluorescence was observed with an EC_{50} ~ 3 μM, a finding that indicates increasing levels of the test molecule accumulated in *E. coli*. Combined, these experiments effectively established the assay parameters necessary for quantifying the accumulation of molecules within the cytosolic compartment of *E. coli*.

In theory, BAPA should be compatible with any azide-bearing fluorophore as long as the fluorophore is able to reach HaloTag to report on the remaining unclicked DBCO handles.

To test this concept, an azide-bearing fluorescein (**Flaz**) and an azide-bearing coumarin (**Comaz**) were included in a BAPA formatted assay (**Fig. 4G**). Both fluorophores led to a signal increase upon the induction of protein expression with IPTG. As expected, due to its negative charge, the fluorescence increase with **Flaz** was considerably lower than that with **R110az**. To show that the cell wall of *E. coli* remained intact after induction of HaloTag and treatment with **DBCOcl**, we performed a SYTOX Green analysis.[11] In live prokaryotic cells, SYTOX Green is almost entirely excluded from cells with intact permeability barriers.[12] Our results showed that the expression of HaloTag in *E. coli* did not alter the integrity of cell wall (**Fig. S2**).

Appreciating that the assay is effectively complete at the end of pulse step (the incubation with the test molecule), we reasoned that we could reach higher signal-to-noise by removing the permeation barrier to the dye. For *E. coli*, it has been found that formaldehyde fixation can outperform alcohol-based fixation in terms of increasing permeability.[13] Our results showed that fixation prior to the pulse step led to an increase in overall fluorescence levels for all three dyes tested (**Fig. S3**). This suggests that there are still considerable permeation challenges by the dye that are imposed by the intact cell wall of *E. coli*. Of the three dyes, the largest signal-to-noise level was found with **Flaz** treatment, which led to a very significant increase in cellular fluorescence and became the primary analysis method going forward.

The permeation of small molecules in Gram-negative bacteria is predominantly hindered by the outer membrane (OM).[14] Prior efforts have focused on identifying compounds that

can disrupt the OM barrier and serve as antibiotic adjuvants. The primary objective is to enhance the efficacy of antibiotics or bypass resistance mechanisms by co-treatment with small molecule OM permeabilizers. This particular class of compounds includes polymyxin B, a Gram-negative specific antibiotic, with its nonapeptide fragment known as polymyxin B nonapeptide (PMBN).[15] PMBN lacks the fatty acid tail but exhibits permeabilizing properties at non-toxic concentrations to bacterial cells. At 5 and 10 μM of PMBN, the colony forming unit (CFU) count was similar to that of untreated cells, a finding that is consistent with literature precedence in the lack of toxicity at these concentrations (**Fig. S4**).[16] Notably, PMBN has shown potential in protecting mice against Gram-negative bacteria when administered alongside erythromycin.[17]

Given our results with formaldehyde fixation, we wondered if BAPA could be leveraged to report on OM permeabilizers. More specifically, we sought to use a dye that should inherently have a low level of cellular permeability. For this series, we focused on the sulfonated cyanine series bearing an azide group, **Cy5az** and **Cy3az**, which would be expected to display low permeability owing to the sulfonate groups (**Fig. 5A**). As before, HaloTag expressing *E. coli* cells were treated with **DBCOcl**. To test the permeabilizabilityof the OM, unfixed cells were either pre-incubated or co-incubated with sub-lethal concentration of PMBN. Our data clearly showed that there was a 19-fold increase in cellular fluorescence when PMBN was pre-incubated with the cells and a 34-fold increase in cellular fluorescence when PMBN was co-incubated with **Cy5az** (**Fig. 5A**). A full range of permeabilization by PMBN was observed by 2.5 μM with an EC_{50} of 0.8 μM (**Fig. S5**). A similar pattern was also observed with the similarly structured

fluorophore **Cy3az**, which indicates that there is permeabilization of the OM upon PMBN treatment with less hydrophobic dyes as well (**Fig. 5B**). Given the large dynamic range, we pose that the assay could be adopted to operate using a plate reader. Our results showed that the dynamic range was mostly maintained in this format (**Fig. S6**), which should provide a more direct path to screening campaigns with diverse molecular libraries.

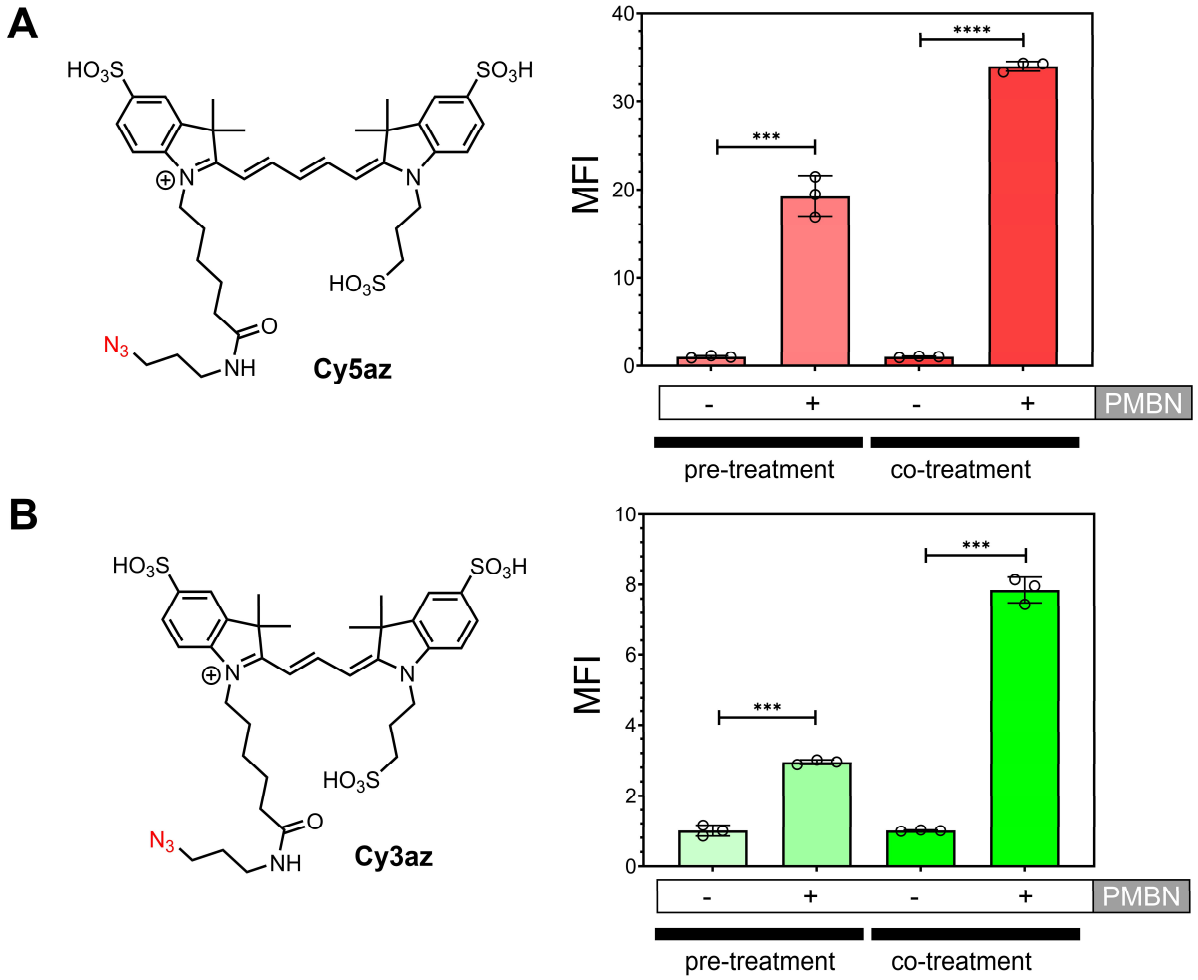

Figure 5. (**A**) Chemical structure of **Cy5az** and flow cytometry analysis of *E. coli* in the presence/absence of **PMBN**. The dye was either co-incubated with PMBN or pre-incubated with **PMBN** for 30 min. (**B**) Chemical structure of **Cy3az** and flow cytometry

analysis of *E. coli* in the presence/absence of **PMBN**. The dye was either co-incubated with PMBN or pre-incubated with **PMBN** as described. Data are represented as mean +/- SD (n = 3 independent samples in a single experiment). *P*-values were determined by a two-tailed *t*-test (*** denotes a *p*-value < 0.001, **** < 0.0001).

We next set out to determine the apparent permeability profile of a diverse set of small molecules. For this set of experiments, a library of 24 commercially available azide-bearing molecules was compiled (**Fig. 6A**). The molecules covered a range of hydrophobicity, rigidity, hydrogen bond donors/acceptors, molecular weight, charge, and polarity. Our results showed that cellular fluorescence levels covered a wide range including some that resulted in a complete reduction in signal (**Fig. 6B**). Appreciating that the azide-group is found in a range of steric and electronic configurations, we wondered if those chemical features could also alter the reactivity with DBCO. In order to assess the reactivity level of the DBCO-azide reaction within the designated timeframe of the assay, we empirically measured the reaction level using DBCO terminated beads (**Fig. S7**). Given the size of these beads, they were also compatible with flow cytometry analysis. A near identical workflow to live cell analysis was performed albeit without the permeability barriers associated with the outer and inner membranes. Interestingly, not all azides reacted within the timescale of the assay and this suggests that azide reactivity will have to be considered. Variability in reactivity profiles has been observed previously between azides and strained alkynes, including DBCO.[18]

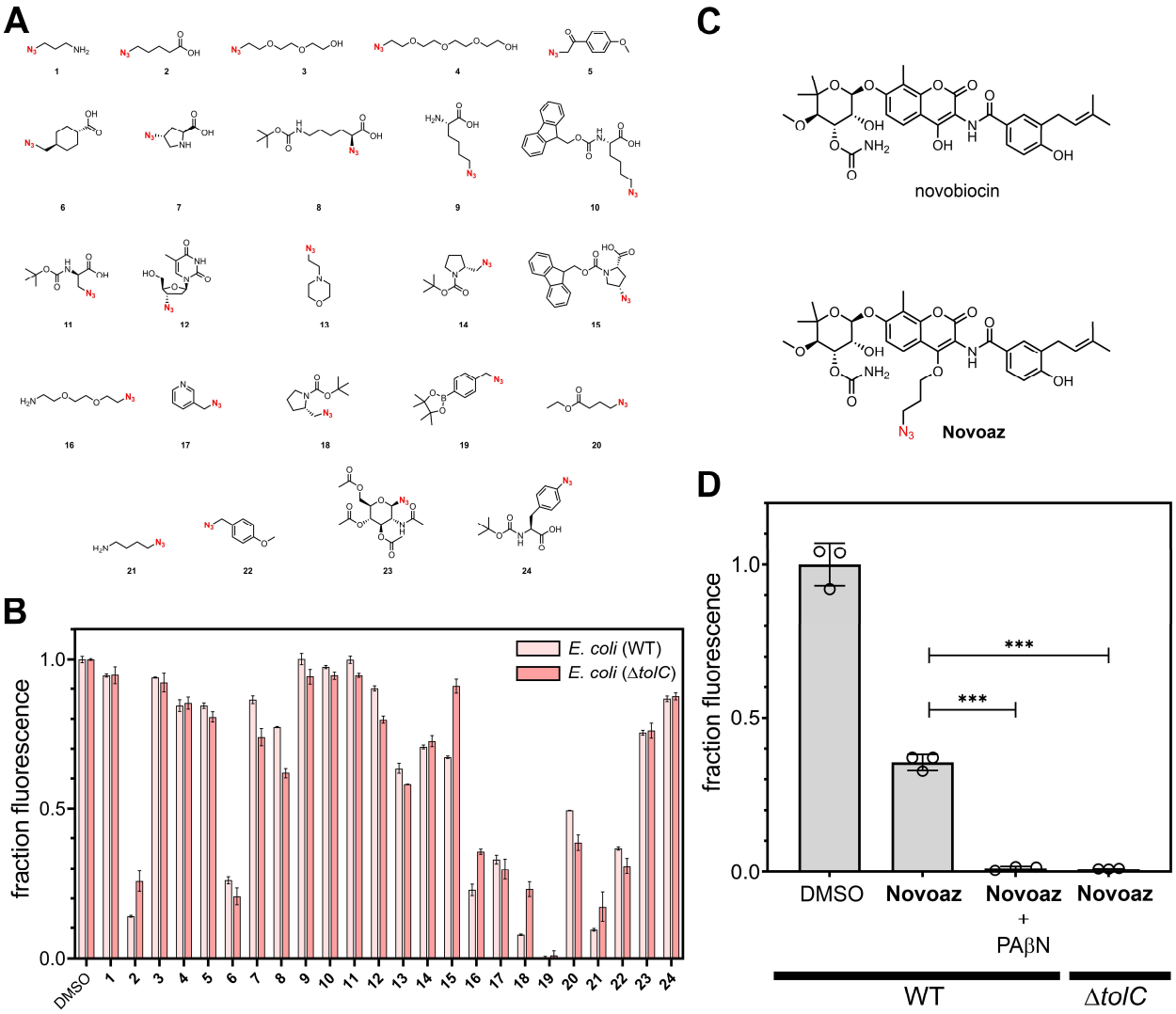

Figure 6. (**A**) Chemical structures of compounds 1-24 that bear an azide tag to be used with BAPA. (**B**) Flow cytometry BAPA analysis of *E. coli* treated with stated compounds in WT and *ΔtolC* followed by **R110az** in the chase step. (**C**) Chemical structures of novobiocin and **Novoaz**. (**D**) Flow cytometry BAPA analysis of *E. coli* WT or *ΔtolC* strains. Cells were treated with 50 μM of **Novoaz** or co-incubated **Novoaz** with PAβN. Data are represented as mean +/- SD (n = 3 independent samples in a single experiment). *P*-values were determined by a two-tailed *t*-test (*** denotes a *p*-value < 0.001).

The challenges posed by the variable reactivity of azides prompted us to consider an alternative approach. To eliminate the impact of the azide reactivity, a differential scan was conceived in which the same molecules are evaluated in two similar strains with a phenotypic difference. The change in apparent permeability, therefore, should isolate the impact to the phenotype. We considered that this would be an appropriate method to establish molecular determinants for recognition by an efflux pump.[19] Efflux pumps can greatly reduce the concentrations of antibiotics by excreting them to the extracellular space. Of the 36 known or putative efflux pumps in *E. coli*,[19] ArcAB-TolC is the best characterized efflux pump and has been described as the most prevalent in decreasing susceptibility to antibiotics.[20] Genetic deletion of *tolC* is sufficient to disrupt the tripartite formation of the ArcAB-TolC complex.[21] In our assay, WT *E. coli* cells and *tolC*-null *E. coli* cells were evaluated using the 24-member panel of compounds. Additionally, these cells overexpressed the porin FhuA, which is a commonly used strategy aimed at increasing permeability of *E. coli*.[22] The rationale for using a hyper-porinated strain is to effectively increase the likelihood that compounds are able to reach the cytosol, where they can potentially get recognized by ArcAB-TolC. We expect that molecules that are recognized and actively excreted from the cytosol by ArcAB-TolC will lead to higher fluorescence levels. Our results showed that there are a number of molecules that had significantly decreased fluorescence upon *tolC* deletion, suggesting that they are substrates of ArcAB-TolC (**Fig. 6B**).

To further confirm the ability of the assay to establish structural recognition by efflux pumps, we adopted an antibiotic that has been previously described as a canonical substrate of ArcAB-TolC. Novobiocin is a type of antibiotic that belongs to the class of aminocoumarin antibiotics and it inhibits bacterial DNA gyrase (**Fig. 6C**).[23] Given its cytosolic target, novobiocin needs to permeate past the OM and reach the target gyrase. Deletion and mutations to *tolC* can dramatically alter the MIC of novobiocin, which has been ascribed to its substrate recognition.[24] An azide-modified novobiocin derivative was synthesized that minimally altered the chemical configuration of the original antibiotic (**Fig. 6C** and **SI Scheme 2**). In WT *E. coli*, there was a decrease in cellular fluorescence when cells were subjected to BAPA in the presence of **Novoaz** (**Fig. 6D**), which is an indication that there was some accumulation in the cytosol. The function of TolC can be disrupted with small molecule inhibitors such as phenylalanine-arginine β-naphthylamide (PAβN).[25] Upon the co-treatment with PAβN, cellular fluorescence was near background consistent with higher retention of **Novoaz** in the cytosol (**Fig. 6D**). Similarly, cellular fluorescence levels were near background in *E. coli* cells without a functional ArcAB-TolC system. Together, these experiments show that **Novoaz** is a substrate of ArcAB-TolC and using BAPA in combination with **Novoaz** may be leveraged to directly screen for true inhibitors of this efflux pump, and potentially others, decoupled from MIC analysis.

To further expand on the chemical space probed for recognition by TolC, we vastly expanded the library set from 24 to 1200 compounds. The Dong and Sharpless groups recently unveiled a novel approach to install azide tags onto molecules using a diazotizing reagent.[26] In doing so, they assembled a large library of molecules that are compatible

with BAPA. First, we tested the robustness of BAPA in a 96-well plate format to project its compatibility with a high-throughput analysis platform using a positive and negative control from the 24-member library. Three compounds were included that spanned high levels of cellular fluorescence, low levels of cellular fluorescence, and one in between. For each of these three compounds, they were repeated across 96 wells to test the reproducibility of these measurements. From these experiments, it was clear that the assay was highly reproducible and had a high Z' score of 0.954 (**Fig. 7A**). Next, we applied BAPA to the entire set of 1200 molecules both in *E. coli* and Δ*tolC E. coli* with the goal of more precisely defining the molecular determinants of substrate recognition by ArcAB-TolC. From our results, it is clear that a number of molecules had lower fluorescence levels in the TolC-null strains, and this suggests that they are substrates for ArcAB-TolC (**Fig. 7A**). Indeed, 293 compounds demonstrated a 5% change in fluorescence, 98 compounds had a 10% difference, and 16 compounds had a difference of 20%.

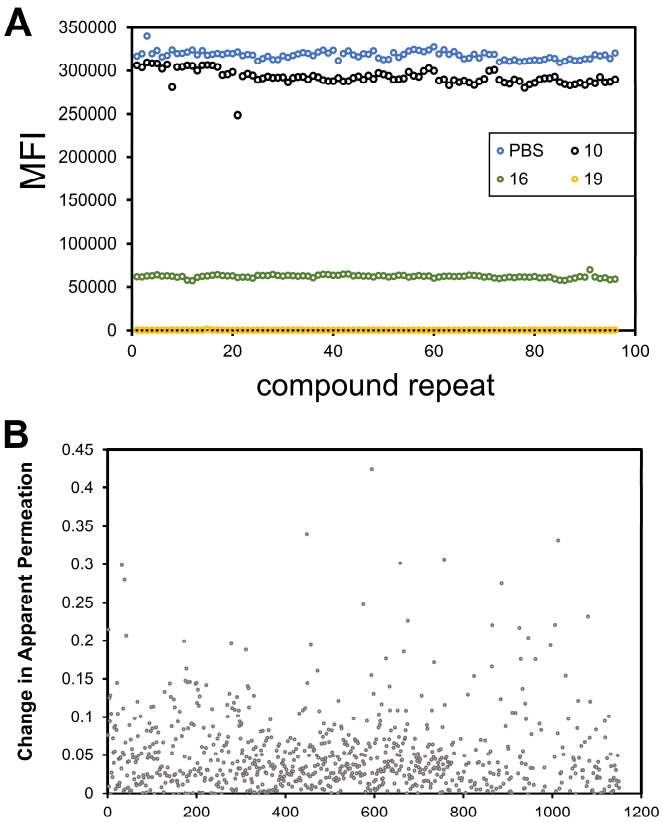

Figure 7. (**A**) Flow cytometry BAPA analysis of WT *E. coli* treated with stated compounds selected from the 24-member library followed by **R110az** in the chase step using a 96-well plate. (**B**) Flow cytometry BAPA analysis of *E. coli* treated with 1200 compounds in WT and *ΔtolC* strains followed by **R110az** in the chase step using a 96-well plate.

Discussion

Due to the limited availability of effective treatment options, projections suggest that by 2050, the number of fatalities caused by antibiotic-resistant infections will surpass those caused by cancer.[27] Our ability to combat infections will be increasingly compromised as the prevalence of drug-resistant bacteria continues to rise. Furthermore, the ineffectiveness of antibiotics undermines significant advancements in medical procedures

such as organ transplants, invasive surgeries, and cancer chemotherapy, all of which heavily rely on these medications for their success. To maintain the standards of medical care, it is imperative that we reinvest in overcoming the critical obstacles in antibiotic drug discovery. One major challenge in discovering new agents lies in the limited ability of small molecules to penetrate Gram-negative bacteria.

In developing BAPA, our laboratory leveraged the efficient and selective reaction of HaloTag with chloroalkane-modified molecules. Prior efforts using HaloTag in bacteria focused on the tracking of protein fusions[28] and the role of cationic peptides on membrane permeabilization.[29] Building on these precedents, our laboratory recently developed the BaCAPA to measure the apparent accumulation of molecules into bacterial cells.[7] For BAPA, the test molecule is modified with an azide epitope instead of a chloroalkane linker. In this assay workflow, *E. coli* are pre-treated with DBCO-modified chloroalkane to anchor a strained alkyne to HaloTag followed by incubation with azide-bearing test molecules. Cells are subsequently subjected to a chase step with an azide-tagged fluorophore, which will react with the leftover unmodified DBCO epitopes. Therefore, a decrease in cellular fluorescence signal reflects apparent high levels of accumulation of the test molecule into bacterial cells.

The intracellular reaction of azide and DBCO is expected to be orthogonal to other biomacromolecules in the cytosol of bacteria and, in general, be completed relatively fast. The Fox laboratory found that the reaction between DBCO and azide inside mammalian cells was complete within 30 minutes ($t_{1/2}$ of ~ 5 min) using TAMRA-azide.[30] Further

showing feasibility, a group at Novartis anchored DBCO in the cell walls of *E. coli*; however, in their iteration the triazole products were quantitated by MS, limiting the analysis to less than five molecules.[9] Our own laboratory recently described the combination of DBCO-azide to determine the accessibility of molecules to and within *Staphylococcus aureus* peptidoglycan[31] and successfully miniaturized the assay for high-throughput analysis of a transposon library using 384-well plates.[32] Most relevantly, our own laboratory recently demonstrated that the combination of DBCO (metabolically anchored onto the peptidoglycan) and azide-tagged test molecules can report on permeability of small molecules across the 'myco' membrane of Mycobacteria, including in the causative agent of tuberculosis.[33]

For antibiotics that do not manage to cross the OM efficiently, an alternative strategy may be the co-treatment with an adjuvant molecule that disrupts the OM thus promoting the passage of molecules to their molecular target. The most commonly utilized OM permealizer is PMBN, a fragment of the colistin family of antibiotics. Our results showed that the OM is clearly the primary barrier for permeability as its disruption led to significant increase in fluorescence by an azide-tagged dye in an IPTG-dependent manner. Intriguingly, the pre-treatment of cells with PMBN indicates that the disruption to the integrity of the OM of *E. coli* can persist beyond the point that PMBN is washed away. This indicates that the dye reaches cytosolic space despite the additional inner membrane potentially posing as a permeability barrier. Most importantly, we demonstrated that BAPA can analyze the ability of molecules to permeabilize the OM of *E. coli* by directly measuring increased permeability of other highly impermeable molecules. Given the

ability to adapt the assay to a plate reading format, we will explore in the future how it can be implemented in a high-throughput screen campaign for novel OM permeabilizers.

For molecules that navigate past the OM, the next challenge is retention. In drug-resistant bacteria, efflux pumps can reduce the accumulation of molecules that are structurally unrelated.[19, 34, 35] While it is generally understood that efflux pumps often play an important role in drug resistant phenotypes, it remains poorly defined how molecular structure drives recognition by efflux pumps. Most FDA-approved antibiotics are hydrophilic compounds that are proposed to penetrate outer membranes *via* porins.[36] Assignment of substrates to specific efflux pumps has been made primarily by correlative analysis between expression levels and antibiotic susceptibility. Antibiotic susceptibility correlations have many disadvantages that can lead to mis-assignments. The deletion of porins can be a valuable tool to study recognition of substrates. We showed that BAPA can be used in combination with the deletion of a primary efflux pump, ArcAB-TolC, to comprehensively test a large library of molecules for their potential recognition. In the future we plan to start with EKO-35, a strain that has 35 of the efflux pumps deleted out of the genome,[37] and then compare this strain to one in which a single efflux pump is introduced. This method will allow for the more precise assignment of structural preference among the various efflux pumps in *E. coli*.

While the primary focus on our study was recognition by an efflux pump, we project that a similar approach can be applied to decipher the molecular profile of molecules that reach the periplasmic space by traversing through OM-imbedded porins.[35] The passage

of antibiotics through porins in Gram-negative bacteria is influenced by factors such as the size, charge, and hydrophilicity of the molecule as well as the properties of the porins themselves. The importance of porins for small molecule permeation is exemplified by the overexpression of the outer membrane siderophore FhuA, which effectively acts like an open and nonselective porin for the uptake of molecules.[22] Hyper-porinated *E. coli* become highly susceptible to large antibiotics like vancomycin (MIC 1 μg/mL vs. 128 μg/mL for WT), novobiocin, and erythromycin.

Conclusion

Gram-negative bacteria, such as *E. coli*, have an outer membrane and an inner plasma membrane that act as formidable barriers that severely restrict the movement of molecules into and out of the cell. The selective permeability of these membranes can make it challenging for antibiotics to reach intracellular targets. Being able to readily measure intracellular accumulation levels could potentially expedite drug discovery and development. Yet, this type of analysis continues to be a major challenge for the field. We describe a novel platform, BAPA, that effectively converts HaloTag expressed in the cytosol of *E. coli* to a strained alkyne. Test molecules tagged with an azide group are imprinted onto HaloTag if they arrive within the cytosol. As a final step, the level of accumulation is defined by the level of unoccupied sites with an azide-tagged fluorophore. We demonstrated that fluorescence can be readily measured by flow cytometry or standard plate reader analysis, making it compatible with high throughput screens. The robustness of the assay was confirmed empirically, and the throughput was exemplified

by screening over 2000 individual test molecules. In addition, we demonstrated that BAPA can be deployed to report on OM permeabilizers, and we are currently using it to screen for adjuvants that increase the accumulation levels of antibiotics. Finally, we showed that BAPA can be used to describe molecular profiles that increase recognition by the efflux pump ArcAB-TolC.

Acknowledgement

This study was supported by the NIH grant GM124893-01 (M.M.P.).

Supporting Information

Additional figures, tables, and materials/methods are included in the supporting information file.

References

(1) Brown, D. G.; May-Dracka, T. L.; Gagnon, M. M.; Tommasi, R. Trends and exceptions of physical properties on antibacterial activity for Gram-positive and Gram-negative pathogens. *J Med Chem* **2014**, *57* (23), 10144-10161. DOI: 10.1021/jm501552x. O'Shea, R.; Moser, H. E. Physicochemical properties of

antibacterial compounds: implications for drug discovery. *J Med Chem* **2008**, *51* (10), 2871-2878. DOI: 10.1021/jm700967e.

(2) Kojima, S.; Nikaido, H. Permeation rates of penicillins indicate that Escherichia coli porins function principally as nonspecific channels. *Proc Natl Acad Sci U S A* **2013**, *110* (28), E2629-2634. DOI: 10.1073/pnas.1310333110

1310333110 [pii]. June, C. M.; Vaughan, R. M.; Ulberg, L. S.; Bonomo, R. A.; Witucki, L. A.; Leonard, D. A. A fluorescent carbapenem for structure function studies of penicillin-binding proteins, beta-lactamases, and beta-lactam sensors. *Anal Biochem* **2014**, *463*, 70-74. DOI: 10.1016/j.ab.2014.07.012

S0003-2697(14)00306-6 [pii]. Zhou, Y.; Joubran, C.; Miller-Vedam, L.; Isabella, V.; Nayar, A.; Tentarelli, S.; Miller, A. Thinking outside the "bug": a unique assay to measure intracellular drug penetration in gram-negative bacteria. *Anal Chem* **2015**, *87* (7), 3579-3584. DOI: 10.1021/ac504880r. Davis, T. D.; Gerry, C. J.; Tan, D. S. General platform for systematic quantitative evaluation of small-molecule permeability in bacteria. *ACS Chem Biol* **2014**, *9* (11), 2535-2544. DOI: 10.1021/cb5003015. Cama, J.; Bajaj, H.; Pagliara, S.; Maier, T.; Braun, Y.; Winterhalter, M.; Keyser, U. F. Quantification of Fluoroquinolone Uptake through the Outer Membrane Channel OmpF of Escherichia coli. *J Am Chem Soc* **2015**, *137* (43), 13836-13843. DOI: 10.1021/jacs.5b08960. Ghai, I.; Winterhalter, M.; Wagner, R. Probing transport of charged beta-lactamase inhibitors through OmpC, a membrane channel from E. coli. *Biochem Biophys Res Commun* **2017**, *484* (1), 51-55. DOI: S0006-291X(17)30126-2 [pii]

10.1016/j.bbrc.2017.01.076. Kascakova, S.; Maigre, L.; Chevalier, J.; Refregiers, M.; Pages, J. M. Antibiotic transport in resistant bacteria: synchrotron UV fluorescence microscopy to determine antibiotic accumulation with single cell resolution. *PLoS One* **2012**, *7* (6), e38624. DOI: 10.1371/journal.pone.0038624. Cinquin, B.; Maigre, L.; Pinet, E.; Chevalier, J.; Stavenger, R. A.; Mills, S.; Refregiers, M.; Pages, J. M. Microspectrometric insights on the uptake of antibiotics at the single bacterial cell level. *Sci Rep* **2015**, *5*, 17968. DOI: 10.1038/srep17968
srep17968 [pii].

(3) Richter, M. F.; Drown, B. S.; Riley, A. P.; Garcia, A.; Shirai, T.; Svec, R. L.; Hergenrother, P. J. Predictive compound accumulation rules yield a broad-spectrum antibiotic. *Nature* **2017**, *545* (7654), 299-304. DOI: 10.1038/nature22308.

(4) Mientkiewicz, K. M.; Peraro, L.; Kritzer, J. A. Parallel Screening Using the Chloroalkane Penetration Assay Reveals Structure-Penetration Relationships. *ACS Chem Biol* **2021**, *16* (7), 1184-1190. DOI: 10.1021/acschembio.1c00434. Peraro, L.; Deprey, K. L.; Moser, M. K.; Zou, Z.; Ball, H. L.; Levine, B.; Kritzer, J. A. Cell Penetration Profiling Using the Chloroalkane Penetration Assay. *J Am Chem Soc* **2018**, *140* (36), 11360-11369. DOI: 10.1021/jacs.8b06144. Deprey, K.; Kritzer, J. A. Quantitative measurement of cytosolic penetration using the chloroalkane penetration assay. *Methods Enzymol* **2020**, *641*, 277-309. DOI: 10.1016/bs.mie.2020.03.003.

(5) Los, G. V.; Wood, K. The HaloTag: a novel technology for cell imaging and protein analysis. *Methods Mol Biol* **2007**, *356*, 195-208. DOI: 10.1385/1-59745-217-3:195. Los, G. V.; Encell, L. P.; McDougall, M. G.; Hartzell, D. D.; Karassina, N.; Zimprich, C.; Wood, M. G.; Learish, R.; Ohana, R. F.; Urh, M.; et al. HaloTag: a novel protein labeling

technology for cell imaging and protein analysis. *ACS Chem Biol* **2008**, *3* (6), 373-382. DOI: 10.1021/cb800025k. Hoelzel, C. A.; Zhang, X. Visualizing and Manipulating Biological Processes by Using HaloTag and SNAP-Tag Technologies. *Chembiochem* **2020**, *21* (14), 1935-1946. DOI: 10.1002/cbic.202000037. England, C. G.; Luo, H.; Cai, W. HaloTag technology: a versatile platform for biomedical applications. *Bioconjug Chem* **2015**, *26* (6), 975-986. DOI: 10.1021/acs.bioconjchem.5b00191. Benink, H. A.; Urh, M. HaloTag technology for specific and covalent labeling of fusion proteins. *Methods Mol Biol* **2015**, *1266*, 119-128. DOI: 10.1007/978-1-4939-2272-7_8.

(6) Brown, H.; Chung, M.; Uffing, A.; Batistatou, N.; Tsang, T.; Doskocil, S.; Mao, W.; Willbold, D.; Bast, R. C., Jr.; Lu, Z.; et al. Structure-Based Design of Stapled Peptides That Bind GABARAP and Inhibit Autophagy. *J Am Chem Soc* **2022**, *144* (32), 14687-14697. DOI: 10.1021/jacs.2c04699. Cerulli, R. A.; Shehaj, L.; Tosic, I.; Jiang, K.; Wang, J.; Frank, D. A.; Kritzer, J. A. Cytosolic delivery of peptidic STAT3 SH2 domain inhibitors. *Bioorg Med Chem* **2020**, *28* (12), 115542. DOI: 10.1016/j.bmc.2020.115542. Dai, S. A.; Hu, Q.; Gao, R.; Blythe, E. E.; Touhara, K. K.; Peacock, H.; Zhang, Z.; von Zastrow, M.; Suga, H.; Shokat, K. M. State-selective modulation of heterotrimeric Galphas signaling with macrocyclic peptides. *Cell* **2022**, *185* (21), 3950-3965 e3925. DOI: 10.1016/j.cell.2022.09.019. Deprey, K.; Batistatou, N.; Debets, M. F.; Godfrey, J.; VanderWall, K. B.; Miles, R. R.; Shehaj, L.; Guo, J.; Andreucci, A.; Kandasamy, P.; et al. Quantitative Measurement of Cytosolic and Nuclear Penetration of Oligonucleotide Therapeutics. *ACS Chem Biol* **2022**, *17* (2), 348-360. DOI: 10.1021/acschembio.1c00830. Foley, C. A.; Potjewyd, F.; Lamb, K. N.; James, L. I.; Frye, S. V. Assessing the Cell Permeability of Bivalent Chemical Degraders Using the

Chloroalkane Penetration Assay. *ACS Chem Biol* **2020**, *15* (1), 290-295. DOI: 10.1021/acschembio.9b00972. Friedman Ohana, R.; Levin, S.; Hurst, R.; Rosenblatt, M. M.; Zimmerman, K.; Machleidt, T.; Wood, K. V.; Kirkland, T. A. Streamlined Target Deconvolution Approach Utilizing a Single Photoreactive Chloroalkane Capture Tag. *ACS Chem Biol* **2021**, *16* (2), 404-413. DOI: 10.1021/acschembio.0c00987. Gallagher, E. E.; Menon, A.; Chmiel, A. F.; Deprey, K.; Kritzer, J. A.; Garner, A. L. A cell-penetrant lactam-stapled peptide for targeting eIF4E protein-protein interactions. *Eur J Med Chem* **2020**, *205*, 112655. DOI: 10.1016/j.ejmech.2020.112655. Gray, J. P.; Uddin, M. N.; Chaudhari, R.; Sutton, M. N.; Yang, H.; Rask, P.; Locke, H.; Engel, B. J.; Batistatou, N.; Wang, J.; et al. Directed evolution of cyclic peptides for inhibition of autophagy. *Chem Sci* **2021**, *12* (10), 3526-3543. DOI: 10.1039/d0sc03603j. Haberman, V. A.; Fleming, S. R.; Leisner, T. M.; Puhl, A. C.; Feng, E.; Xie, L.; Chen, X.; Goto, Y.; Suga, H.; Parise, L. V.; et al. Discovery and Development of Cyclic Peptide Inhibitors of CIB1. *ACS Med Chem Lett* **2021**, *12* (11), 1832-1839. DOI: 10.1021/acsmedchemlett.1c00438. Klein, V. G.; Townsend, C. E.; Testa, A.; Zengerle, M.; Maniaci, C.; Hughes, S. J.; Chan, K. H.; Ciulli, A.; Lokey, R. S. Understanding and Improving the Membrane Permeability of VH032-Based PROTACs. *ACS Med Chem Lett* **2020**, *11* (9), 1732-1738. DOI: 10.1021/acsmedchemlett.0c00265. Lopez-Andarias, J.; Saarbach, J.; Moreau, D.; Cheng, Y.; Derivery, E.; Laurent, Q.; Gonzalez-Gaitan, M.; Winssinger, N.; Sakai, N.; Matile, S. Cell-Penetrating Streptavidin: A General Tool for Bifunctional Delivery with Spatiotemporal Control, Mediated by Transport Systems Such as Adaptive Benzopolysulfane Networks. *J Am Chem Soc* **2020**, *142* (10), 4784-4792. DOI: 10.1021/jacs.9b13621. Martinent, R.; Du, D.; Lopez-Andarias, J.; Sakai, N.; Matile, S.

Oligomers of Cyclic Oligochalcogenides for Enhanced Cellular Uptake. *Chembiochem* **2021**, *22* (1), 253-259. DOI: 10.1002/cbic.202000630. Martinent, R.; Tawffik, S.; Lopez-Andarias, J.; Moreau, D.; Laurent, Q.; Matile, S. Dithiolane quartets: thiol-mediated uptake enables cytosolic delivery in deep tissue. *Chem Sci* **2021**, *12* (41), 13922-13929. DOI: 10.1039/d1sc04828g. Peraro, L.; Zou, Z.; Makwana, K. M.; Cummings, A. E.; Ball, H. L.; Yu, H.; Lin, Y. S.; Levine, B.; Kritzer, J. A. Diversity-Oriented Stapling Yields Intrinsically Cell-Penetrant Inducers of Autophagy. *J Am Chem Soc* **2017**, *139* (23), 7792-7802. DOI: 10.1021/jacs.7b01698. Rajabi, N.; Hansen, T. N.; Nielsen, A. L.; Nguyen, H. T.; Baek, M.; Bolding, J. E.; Bahlke, O. O.; Petersen, S. E. G.; Bartling, C. R. O.; Stromgaard, K.; et al. Investigation of Carboxylic Acid Isosteres and Prodrugs for Inhibition of the Human SIRT5 Lysine Deacylase Enzyme. *Angew Chem Int Ed Engl* **2022**, *61* (22), e202115805. DOI: 10.1002/anie.202115805. Shin, M. K.; Hyun, Y. J.; Lee, J. H.; Lim, H. S. Comparison of Cell Permeability of Cyclic Peptoids and Linear Peptoids. *ACS Comb Sci* **2018**, *20* (4), 237-242. DOI: 10.1021/acscombsci.7b00194. Wang, H. M.; Seo, C. D.; Lee, K. J.; Park, J. H.; Lim, H. S. Evaluation of the cell permeability of bicyclic peptoids and bicyclic peptide-peptoid hybrids. *Bioorg Chem* **2022**, *127*, 105976. DOI: 10.1016/j.bioorg.2022.105976. Yin, H.; Huang, Y. H.; Deprey, K.; Condon, N. D.; Kritzer, J. A.; Craik, D. J.; Wang, C. K. Cellular Uptake and Cytosolic Delivery of a Cyclic Cystine Knot Scaffold. *ACS Chem Biol* **2020**, *15* (6), 1650-1661. DOI: 10.1021/acschembio.0c00297. Yoo, D. Y.; Barros, S. A.; Brown, G. C.; Rabot, C.; Bar-Sagi, D.; Arora, P. S. Macropinocytosis as a Key Determinant of Peptidomimetic Uptake in Cancer Cells. *J Am Chem Soc* **2020**, *142* (34), 14461-14471. DOI: 10.1021/jacs.0c02109. Yu, J. J.; Zhou, D. D.; Yang, X. X.; Cui, B.; Tan, F. W.; Wang, J.;

Li, K.; Shang, S.; Zhang, C.; Lv, X. X.; et al. TRIB3-EGFR interaction promotes lung cancer progression and defines a therapeutic target. *Nat Commun* **2020**, *11* (1), 3660. DOI: 10.1038/s41467-020-17385-0.

(7) Ongwae, G. M.; Lepori, I.; Chordia, M. D.; Dalesandro, B. E.; Apostolos, A. J.; Siegrist, M. S.; Pires, M. M. Measurement of Small Molecule Accumulation into Diderm Bacteria. *ACS Infect Dis* **2023**, *9* (1), 97-110. DOI: 10.1021/acsinfecdis.2c00435 From NLM Medline.

(8) Jewett, J. C.; Bertozzi, C. R. Cu-free click cycloaddition reactions in chemical biology. *Chem Soc Rev* **2010**, *39* (4), 1272-1279. DOI: 10.1039/b901970g From NLM Medline. Agard, N. J.; Prescher, J. A.; Bertozzi, C. R. A strain-promoted [3 + 2] azide-alkyne cycloaddition for covalent modification of biomolecules in living systems. *J Am Chem Soc* **2004**, *126* (46), 15046-15047. DOI: 10.1021/ja044996f From NLM Medline.

(9) Spangler, B.; Dovala, D.; Sawyer, W. S.; Thompson, K. V.; Six, D. A.; Reck, F.; Feng, B. Y. Molecular Probes for the Determination of Subcellular Compound Exposure Profiles in Gram-Negative Bacteria. *ACS Infect Dis* **2018**, *4* (9), 1355-1367. DOI: 10.1021/acsinfecdis.8b00093. Spangler, B.; Yang, S.; Baxter Rath, C. M.; Reck, F.; Feng, B. Y. A Unified Framework for the Incorporation of Bioorthogonal Compound Exposure Probes within Biological Compartments. *ACS Chem Biol* **2019**, *14* (4), 725-734. DOI: 10.1021/acschembio.9b00008.

(10) Feigman, M. S.; Kim, S.; Pidgeon, S. E.; Yu, Y.; Ongwae, G. M.; Patel, D. S.; Regen, S.; Im, W.; Pires, M. M. Synthetic Immunotherapeutics against Gram-negative Pathogens. *Cell Chem Biol* **2018**, *25* (10), 1185-1194 e1185. DOI: 10.1016/j.chembiol.2018.05.019. Lee, J.; Patel, D. S.; Kucharska, I.; Tamm, L. K.; Im,

W. Refinement of OprH-LPS Interactions by Molecular Simulations. *Biophys J* **2017**, *112* (2), 346-355. DOI: 10.1016/j.bpj.2016.12.006.

(11) Mortimer, F. C.; Mason, D. J.; Gant, V. A. Flow cytometric monitoring of antibiotic-induced injury in Escherichia coli using cell-impermeant fluorescent probes. *Antimicrob Agents Chemother* **2000**, *44* (3), 676-681. DOI: 10.1128/AAC.44.3.676-681.2000 From NLM Medline.

(12) Roth, B. L.; Poot, M.; Yue, S. T.; Millard, P. J. Bacterial viability and antibiotic susceptibility testing with SYTOX green nucleic acid stain. *Appl Environ Microbiol* **1997**, *63* (6), 2421-2431. DOI: 10.1128/aem.63.6.2421-2431.1997 From NLM Medline.

(13) Zhu, L.; Rajendram, M.; Huang, K. C. Effects of fixation on bacterial cellular dimensions and integrity. *iScience* **2021**, *24* (4), 102348. DOI: 10.1016/j.isci.2021.102348 From NLM PubMed-not-MEDLINE.

(14) Stokes, J. M.; MacNair, C. R.; Ilyas, B.; French, S.; Cote, J. P.; Bouwman, C.; Farha, M. A.; Sieron, A. O.; Whitfield, C.; Coombes, B. K.; et al. Pentamidine sensitizes Gram-negative pathogens to antibiotics and overcomes acquired colistin resistance. *Nat Microbiol* **2017**, *2*, 17028. DOI: 10.1038/nmicrobiol.2017.28. Klobucar, K.; Cote, J. P.; French, S.; Borrillo, L.; Guo, A. B. Y.; Serrano-Wu, M. H.; Lee, K. K.; Hubbard, B.; Johnson, J. W.; Gaulin, J. L.; et al. Chemical Screen for Vancomycin Antagonism Uncovers Probes of the Gram-Negative Outer Membrane. *ACS Chem Biol* **2021**, *16* (5), 929-942. DOI: 10.1021/acschembio.1c00179. Vaara, M. Agents that increase the permeability of the outer membrane. *Microbiol Rev* **1992**, *56* (3), 395-411. DOI: 10.1128/mr.56.3.395-411.1992. Ejim, L.; Farha, M. A.; Falconer, S. B.; Wildenhain, J.; Coombes, B. K.; Tyers, M.; Brown, E. D.; Wright, G. D. Combinations of antibiotics and

nonantibiotic drugs enhance antimicrobial efficacy. *Nat Chem Biol* **2011**, *7* (6), 348-350. DOI: 10.1038/nchembio.559.

(15) Poirel, L.; Jayol, A.; Nordmann, P. Polymyxins: Antibacterial Activity, Susceptibility Testing, and Resistance Mechanisms Encoded by Plasmids or Chromosomes. *Clin Microbiol Rev* **2017**, *30* (2), 557-596. DOI: 10.1128/CMR.00064-16 From NLM Medline.

(16) French, S.; Farha, M.; Ellis, M. J.; Sameer, Z.; Cote, J. P.; Cotroneo, N.; Lister, T.; Rubio, A.; Brown, E. D. Potentiation of Antibiotics against Gram-Negative Bacteria by Polymyxin B Analogue SPR741 from Unique Perturbation of the Outer Membrane. *ACS Infect Dis* **2020**, *6* (6), 1405-1412. DOI: 10.1021/acsinfecdis.9b00159.

(17) Ofek, I.; Cohen, S.; Rahmani, R.; Kabha, K.; Tamarkin, D.; Herzig, Y.; Rubinstein, E. Antibacterial synergism of polymyxin B nonapeptide and hydrophobic antibiotics in experimental gram-negative infections in mice. *Antimicrob Agents Chemother* **1994**, *38* (2), 374-377. DOI: 10.1128/AAC.38.2.374.

(18) Dommerholt, J.; van Rooijen, O.; Borrmann, A.; Guerra, C. F.; Bickelhaupt, F. M.; van Delft, F. L. Highly accelerated inverse electron-demand cycloaddition of electron-deficient azides with aliphatic cyclooctynes. *Nat Commun* **2014**, *5*, 5378. DOI: 10.1038/ncomms6378 From NLM PubMed-not-MEDLINE.

(19) Du, D.; Wang-Kan, X.; Neuberger, A.; van Veen, H. W.; Pos, K. M.; Piddock, L. J. V.; Luisi, B. F. Multidrug efflux pumps: structure, function and regulation. *Nat Rev Microbiol* **2018**, *16* (9), 523-539. DOI: 10.1038/s41579-018-0048-6 From NLM Medline.

(20) Nishino, K.; Yamaguchi, A. Analysis of a complete library of putative drug transporter genes in Escherichia coli. *J Bacteriol* **2001**, *183* (20), 5803-5812. DOI: 10.1128/JB.183.20.5803-5812.2001 From NLM Medline. Koronakis, V.; Eswaran, J.;

Hughes, C. Structure and function of TolC: the bacterial exit duct for proteins and drugs. *Annu Rev Biochem* **2004**, *73*, 467-489. DOI: 10.1146/annurev.biochem.73.011303.074104 From NLM Medline.

(21) Fralick, J. A. Evidence that TolC is required for functioning of the Mar/AcrAB efflux pump of Escherichia coli. *J Bacteriol* **1996**, *178* (19), 5803-5805. DOI: 10.1128/jb.178.19.5803-5805.1996 From NLM Medline. Gerken, H.; Misra, R. Genetic evidence for functional interactions between TolC and AcrA proteins of a major antibiotic efflux pump of Escherichia coli. *Mol Microbiol* **2004**, *54* (3), 620-631. DOI: 10.1111/j.1365-2958.2004.04301.x From NLM Medline.

(22) Braun, M.; Killmann, H.; Maier, E.; Benz, R.; Braun, V. Diffusion through channel derivatives of the Escherichia coli FhuA transport protein. *Eur J Biochem* **2002**, *269* (20), 4948-4959. DOI: 10.1046/j.1432-1033.2002.03195.x From NLM Medline. Krishnamoorthy, G.; Wolloscheck, D.; Weeks, J. W.; Croft, C.; Rybenkov, V. V.; Zgurskaya, H. I. Breaking the Permeability Barrier of Escherichia coli by Controlled Hyperporination of the Outer Membrane. *Antimicrob Agents Chemother* **2016**, *60* (12), 7372-7381. DOI: 10.1128/AAC.01882-16 From NLM Medline.

(23) Gellert, M.; O'Dea, M. H.; Itoh, T.; Tomizawa, J. Novobiocin and coumermycin inhibit DNA supercoiling catalyzed by DNA gyrase. *Proc Natl Acad Sci U S A* **1976**, *73* (12), 4474-4478. DOI: 10.1073/pnas.73.12.4474 From NLM Medline.

(24) Augustus, A. M.; Celaya, T.; Husain, F.; Humbard, M.; Misra, R. Antibiotic-sensitive TolC mutants and their suppressors. *J Bacteriol* **2004**, *186* (6), 1851-1860. DOI: 10.1128/JB.186.6.1851-1860.2004 From NLM Medline.

(25) Renau, T. E.; Leger, R.; Flamme, E. M.; Sangalang, J.; She, M. W.; Yen, R.; Gannon, C. L.; Griffith, D.; Chamberland, S.; Lomovskaya, O.; et al. Inhibitors of efflux pumps in Pseudomonas aeruginosa potentiate the activity of the fluoroquinolone antibacterial levofloxacin. *J Med Chem* **1999**, *42* (24), 4928-4931. DOI: 10.1021/jm9904598 From NLM Medline.

(26) Meng, G.; Guo, T.; Ma, T.; Zhang, J.; Shen, Y.; Sharpless, K. B.; Dong, J. Modular click chemistry libraries for functional screens using a diazotizing reagent. *Nature* **2019**, *574* (7776), 86-89. DOI: 10.1038/s41586-019-1589-1 From NLM PubMed-not-MEDLINE.

(27) https://amr-review.org/ (accessed.

(28) Ke, N.; Landgraf, D.; Paulsson, J.; Berkmen, M. Visualization of Periplasmic and Cytoplasmic Proteins with a Self-Labeling Protein Tag. *J Bacteriol* **2016**, *198* (7), 1035-1043. DOI: 10.1128/JB.00864-15. Clark, S. A.; Singh, V.; Vega Mendoza, D.; Margolin, W.; Kool, E. T. Light-Up "Channel Dyes" for Haloalkane-Based Protein Labeling in Vitro and in Bacterial Cells. *Bioconjug Chem* **2016**, *27* (12), 2839-2843. DOI: 10.1021/acs.bioconjchem.6b00613.

(29) Yang, Z.; Weisshaar, J. C. HaloTag Assay Suggests Common Mechanism of E. coli Membrane Permeabilization Induced by Cationic Peptides. *ACS Chem Biol* **2018**, *13* (8), 2161-2169. DOI: 10.1021/acschembio.8b00336.

(30) Murrey, H. E.; Judkins, J. C.; Am Ende, C. W.; Ballard, T. E.; Fang, Y.; Riccardi, K.; Di, L.; Guilmette, E. R.; Schwartz, J. W.; Fox, J. M.; et al. Systematic Evaluation of Bioorthogonal Reactions in Live Cells with Clickable HaloTag Ligands: Implications for

Intracellular Imaging. *J Am Chem Soc* **2015**, *137* (35), 11461-11475. DOI: 10.1021/jacs.5b06847.

(31) Ferraro, N. J.; Kim, S.; Im, W.; Pires, M. M. Systematic Assessment of Accessibility to the Surface of Staphylococcus aureus. *ACS Chem Biol* **2021**. DOI: 10.1021/acschembio.1c00604.

(32) Ferraro, N. J.; Pires, M. M. Genetic Determinants of Surface Accessibility in Staphylococcus aureus. *Bioconjug Chem* **2022**, *33* (5), 767-772. DOI: 10.1021/acs.bioconjchem.2c00173.

(33) https://www.biorxiv.org/content/10.1101/2022.10.12.509737v1. Permeation Across the Mycomembrane in Live Mycobacteria. *BioArxiv* **2022**.

(34) Nikaido, H.; Pages, J. M. Broad-specificity efflux pumps and their role in multidrug resistance of Gram-negative bacteria. *FEMS Microbiol Rev* **2012**, *36* (2), 340-363. DOI: 10.1111/j.1574-6976.2011.00290.x. Krishnamoorthy, G.; Leus, I. V.; Weeks, J. W.; Wolloscheck, D.; Rybenkov, V. V.; Zgurskaya, H. I. Synergy between Active Efflux and Outer Membrane Diffusion Defines Rules of Antibiotic Permeation into Gram-Negative Bacteria. *mBio* **2017**, *8* (5). DOI: 10.1128/mBio.01172-17 From NLM Medline.

(35) Pages, J. M.; James, C. E.; Winterhalter, M. The porin and the permeating antibiotic: a selective diffusion barrier in Gram-negative bacteria. *Nat Rev Microbiol* **2008**, *6* (12), 893-903. DOI: 10.1038/nrmicro1994 From NLM Medline.

(36) Isabella, V. M.; Campbell, A. J.; Manchester, J.; Sylvester, M.; Nayar, A. S.; Ferguson, K. E.; Tommasi, R.; Miller, A. A. Toward the rational design of carbapenem uptake in Pseudomonas aeruginosa. *Chem Biol* **2015**, *22* (4), 535-547. DOI: 10.1016/j.chembiol.2015.03.018

S1074-5521(15)00112-X [pii]. Iyer, R.; Sylvester, M. A.; Velez-Vega, C.; Tommasi, R.; Durand-Reville, T. F.; Miller, A. A. Whole-Cell-Based Assay To Evaluate Structure Permeation Relationships for Carbapenem Passage through the Pseudomonas aeruginosa Porin OprD. *ACS Infect Dis* **2017**, *3* (4), 310-319. DOI: 10.1021/acsinfecdis.6b00197. Sugawara, E.; Kojima, S.; Nikaido, H. Klebsiella pneumoniae Major Porins OmpK35 and OmpK36 Allow More Efficient Diffusion of beta-Lactams than Their Escherichia coli Homologs OmpF and OmpC. *J Bacteriol* **2016**, *198* (23), 3200-3208. DOI: JB.00590-16 [pii] 10.1128/JB.00590-16. Tran, Q. T.; Pearlstein, R. A.; Williams, S.; Reilly, J.; Krucker, T.; Erdemli, G. Structure-kinetic relationship of carbapenem antibacterials permeating through E. coli OmpC porin. *Proteins* **2014**, *82* (11), 2998-3012. DOI: 10.1002/prot.24659.

(37) Teelucksingh, T.; Thompson, L. K.; Zhu, S.; Kuehfuss, N. M.; Goetz, J. A.; Gilbert, S. E.; MacNair, C. R.; Geddes-McAlister, J.; Brown, E. D.; Cox, G. A genetic platform to investigate the functions of bacterial drug efflux pumps. *Nat Chem Biol* **2022**, *18* (12), 1399-1409. DOI: 10.1038/s41589-022-01119-y From NLM Medline.